An Acad Bras Cienc (2024) 96(1): e20230971 DOI 10.1590/0001-3765202420230971
Anais da Academia Brasileira de Ciências | *Annals of the Brazilian Academy of Sciences*
Printed ISSN 0001-3765 I Online ISSN 1678-2690
www.scielo.br/aabc | www.fb.com/aabcjournal

BIOMEDICAL SCIENCES

Reactive oxygen species impair Na^+ transport and renal components of the renin-angiotensin-aldosterone system after paraquat poisoning

MARRY A.S. CIRILO, VALÉRIA B.S. SANTOS, NATÁLIA K.S. LIMA, HUMBERTO MUZI-FILHO, ANA D.O. PAIXÃO, ADALBERTO VIEYRA & LEUCIO D. VIEIRA

Abstract: Paraquat (1,1'-dimethyl-4,4'-bipyridyl dichloride) is an herbicide widely used worldwide and officially banned in Brazil in 2020. Kidney lesions frequently occur, leading to acute kidney injury (AKI) due to exacerbated reactive O_2 species (ROS) production. However, the consequences of ROS exposure on ionic transport and the regulator local renin-angiotensin-aldosterone system (RAAS) still need to be elucidated at a molecular level. This study evaluated how ROS acutely influences Na^+-transporting ATPases and the renal RAAS. Adult male Wistar rats received paraquat (20 mg/kg; ip). After 24 h, we observed body weight loss and elevation of urinary flow and serum creatinine. In the renal cortex, paraquat increased ROS levels, NADPH oxidase and (Na^++K^+)ATPase activities, angiotensin II-type 1 receptors, tumor necrosis factor-α (TNF-α), and interleukin-6. In the medulla, paraquat increased ROS levels and NADPH oxidase activity but inhibited (Na^++K^+)ATPase. Paraquat induced opposite effects on the ouabain-resistant Na^+-ATPase in the cortex (decrease) and medulla (increase). These alterations, except for increased serum creatinine and renal levels of TNF-α and interleukin-6, were prevented by 4-hydroxy-2,2,6,6-tetramethylpiperidin-1-oxyl (tempol; 1 mmol/L in drinking water), a stable antioxidant. In summary, after paraquat poisoning, ROS production culminated with impaired medullary function, urinary fluid loss, and disruption of Na^+-transporting ATPases and angiotensin II signaling.

Key words: Acute kidney injury, reactive O_2 species, renal Na^+-transporting ATPases, renin-angiotensin-aldosterone system, tempol.

INTRODUCTION

Paraquat (1,1'-dimethyl-4,4'-bipyridyl dichloride) is a non-selective herbicide still widely used in agricultural crops in vast regions around the world for weed control (Zobiole et al. 2018) and also in non-agriculture areas such as those under electric transmission lines. Since paraquat is highly toxic to mammals, it has been banned in over 50 countries, including Brazil in 2020. For a brief and excellent review regarding the recent history of the herbicide use in Brazil and other countries and the economic implications of its prohibition, see Albrecht et al. (2022).

When ingested, this herbicide causes severe pathological conditions such as acute respiratory syndrome, hepatoxicity, pulmonary fibrosis, cerebral edema, myocardial necrosis, and multiple organ failure (Dinis-Oliveira et al. 2008). Paraquat is not metabolized in the liver, and excretion in its unchanged form occurs in the kidneys (Sukumar et al. 2019). Paraquat acts as a false electron acceptor in the photosystem I in plants, thus generating reactive O_2 species (ROS) and provocating lipid

peroxidation and tissue destruction (Alizadeh et al. 2022). In mammalian organs, such as the lung, liver, kidney, and heart, paraquat interacts with the mitochondrial complexes, leading to intense production of ROS. In the kidney, the herbicide is linked to the onset of severe acute kidney injury (AKI) (Wunnapuk et al. 2013, Tan et al. 2015). However, the molecular mechanisms underpinning this paraquat-induced severe pathology are poorly known.

AKI is characterized by nitrogen waste compounds accumulation and impairment of electrolytes and body fluid homeostasis, resulting from renal function loss (Singh et al. 2012). AKI incidence is 18% in hospitalized patients, increasing to about 70% in intensive care units, with mortality rates ranging from 20% to 70% (Uchino et al. 2005). AKI development is multifactorial; however, most severe cases are frequently associated with acute tubular necrosis of nephrotoxic etiology (Singh et al. 2012). Furthermore, there is increasing evidence that renal tubules are central in the pathogenesis of AKI, as the loss of function leads to secondary glomerular alterations (Chevalier 2016). In addition, higher Na^+ fractional excretion by the failure of proximal reabsorption is linked to poor recovery of renal function and worse prognosis (Moeckel 2018).

Tubular damage is associated with loss of cellular polarity, apoptosis, and necrosis (Havasi & Borkan 2011), impairing fluid reabsorption. The reactive O_2 species (ROS) are pivotal in the onset of renal tubule dysfunction. The proximal tubule has an intense oxidative metabolism (Bełtowski et al. 2007), and its dysfunction leads to fluid wasting because of its importance in fractional reabsorption of filtered fluid. Additionally, oxidative damage in the external medulla can affect Na^+ reabsorption across the thick ascending limb and impact the interstitium hyperosmolality and the urine concentration in the medullary portion of the collecting duct (Rocha & Kokko 1973), thus leading to excessive fluid loss. The tubular reabsorption of fluid depends on the transepithelial Na^+ gradient generated by the primary active basolateral transport of Na^+ mediated by the ouabain-sensitive $(Na^+ + K^+)$ATPase (Féraille & Doucet 2001) and the ouabain-resistant furosemide-sensitive Na^+-ATPase (Rocafull et al. 2011, 2012, Vieyra et al. 2016). The former is responsible for the bulk Na^+ reabsorption, while the latter is associated with its fine-tuning (Bełtowski et al. 2007, Vieira-Filho et al. 2014, Vieyra et al. 2016).

The tissular renin-angiotensin-aldosterone system (RAAS) is a key modulator of the Na^+ reabsorption in the kidney and the extracellular fluid volume (Kobori et al. 2007). Tubulointerstitium levels of angiotensin II (Ang II) are higher than in plasma (Kobori et al. 2007, Wang et al. 2003, Bełtowski et al. 2007), and Na^+-transporting ATPases are tightly regulated by this peptide (Féraille & Doucet 2001, Vieyra et al. 2016). Furthermore, RAAS components are also involved in renal damage in processes in which inflammation and tissue fibrosis are prominent (Kobori et al. 2007). Ang II, the isoform 1 of angiotensin-converting enzyme (ACE1), and the angiotensin II-type 1 receptor (AT_1R) have been linked to inflammation and microvascular dysfunction in ischemia/reperfusion-induced AKI (Da Silveira et al. 2010). The elevated urinary angiotensinogen-creatinine ratio in AKI patients was already positively correlated to adverse outcomes (Alge et al. 2013). Moreover, the RAAS crosstalks with oxidative stress due to increasing ROS production by stimulating NADPH oxidase activity (Sachse & Wolf 2007).

Based on these observations, ROS-mediated alterations of the active Na^+ transport machinery and renal RAAS expression could lead to fluid wasting and depletion of the liquid compartments. This mechanism could

be present in the pathophysiology of several conditions associated with AKI, including herbicide poisoning (Dedeke et al. 2018). This study aimed to investigate whether paraquat-induced ROS generation would lead to changes in cellular and molecular mechanisms able to alter Na^+-transporting ATPases and several renal RAAS components, leading to the development of arterial hypertension.

MATERIALS AND METHODS

Animals

All experimental procedures were approved by the Committee for Ethics in Animal Experimentation at the Federal University of Pernambuco (protocol number 0013/2017) and conducted according to the Brazilian Council of Animal Experimentation (CONCEA) guidelines, which conforms to the provisions of the Declaration of Helsinki (as revised in Brazil in 2013), as well as the NRC Guide for the Care and Use of Laboratory Animals, 8th ed.

Male Wistar rats (300–400 g and approximately 90 days of age) were maintained at 21 ± 3 °C, 12 h:12 h light/dark cycle, and free access to water and standard chow. The rats were submitted to intraperitoneal administration of a single dose of paraquat (20 mg/kg body weight, n = 15; paraquat group, PQ) or vehicle (0.9% NaCl, 1 ml/kg body weight, n = 8; control group, C). Part of the PQ group (n = 7) received 1 mmol/L 4-hydroxy-2,2,6,6-tetramethylpiperidin-1-oxyl (tempol). This free radical scavenger (Ahmed et al. 2014, Youn et al. 2016) was administrated in drinking water for 7 consecutive days before paraquat administration (n = 7; paraquat + tempol group, PQ+T). The rats were randomly distributed in the experimental groups by their sequential distribution. There was no exclusion of animals during the experiment. We chose the dose of paraquat according to a previous study, in which the authors demonstrated that administering this dose induces acute kidney injury and elevation of oxidative stress markers (Tan et al. 2015). The chosen protocol of tempol administration (dose, time, and route) can upregulate antioxidant enzymes and prevent the elevation of oxidative stress induced by kidney injury in rodents (Yoon et al. 2014). For at least one week before paraquat or 0.9% NaCl administration, the rats were acclimated for three consecutive 24-hour periods in metabolic cages. Immediately after paraquat or 0.9% NaCl administration, all animals were placed in individual metabolic cages for 24 h and then submitted to systolic blood pressure (SBP) evaluation. Finally, the rats were anesthetized (ketamine and xylazine; 80 and 10 mg/kg of body weight, respectively, ip) and submitted to a blood sample withdrawn from the abdominal aorta. The kidneys and one liver sample were collected, snap-frozen in liquid N_2, and maintained at −80 °C.

General metabolic and renal function data, and systolic blood pressure

Water and diet intake were also evaluated in the rats housed in metabolic cages, and 24-hour urine samples were collected. Serum and urine creatinine concentrations were measured using a commercial colorimetric kit (Creatinine K, ref: 96; Labtest, Lagoa Santa, Brazil). We also measured serum alanine aminotransferase (ALT) and aspartate aminotransferase (AST) activities in plasma using a commercial colorimetric kit (ALT Liquiform, ref: 109; and AST Liquiform, ref: 108, Labtest), and plasma and urinary protein concentration using the Folin-phenol method (Lowry et al. 1951).

SBP and heart rate (HR) were measured noninvasively in conscious rats using tail-cuff plethysmography (IITC Life Science B60-7/16, Life Science Instruments, Woodland Hills, CA, USA).

The animals were trained for 3 consecutive days in experimental procedures of plethysmography, as described elsewhere (Vieira-Filho et al. 2014).

Lipid peroxidation

Renal (cortex and medulla) and liver samples were homogenized in an ice-cold solution containing 150 mmol/L KCl and 3 mmol/L ethylenediaminetetraacetic acid (EDTA) to evaluate lipid peroxidation. Lipid peroxidation was assessed by measuring thiobarbituric acid reactive substances (TBARS) in tissue homogenates, according to the method of Ohkawa et al. (1979). The TBARS levels were corrected by the protein content of the sample, measured by the Folin-phenol method (Lowry et al. 1951).

In situ levels of reactive O_2 species

ROS levels were evaluated in the renal *cortex corticis* and medulla using the fluorescent superoxide probe dihydroethidium (DHE; Sigma-Aldrich, Saint Louis, MO, USA). The *cortex corticis* was isolated as described by Vieyra et al. (1986). The outermost renal cortex area is where more than 95% of the cell population corresponds to proximal tubule cells (Whittembury & Proverbio 1970). After euthanasia, 3-mm thick renal sections were snap-frozen embedded in optimal cutting temperature (OCT) compound (Sakura Finetek, Terrance, CA, USA) and maintained at -80°C. Next, 5-µm slices were incubated in 100 mmol/L diethylene thiamine-pentaacetic acid (DTPA) solution (in 100 mmol/L phosphate-buffered saline/PBS at pH 7.4) for 30 min and subsequently incubated in 5 µmol/L DHE (in PBS). Finally, the slices were mounted. DHE fluorescence was quantified using fluorescence microscopy (Eclipse Ni-U microscope coupled to camera DS-i, Nikon, Shanghai, China) at 530–560 nm excitation and 590–650 nm emission. The results of each rat were an average fluorescence intensity of 10 cortical and software (version 4.5.1, Media Cybernetics, Rockville, MD, USA).

Superoxide anion ($O_2^{\cdot-}$) formation and NADPH oxidase activity

Renal superoxide anion ($O_2^{\cdot-}$) formation and NADPH oxidase activity were assessed by lucigenin-derived chemiluminescence according to the method previously described (Lima et al. 2021). The *cortex corticis* and medulla samples were separated and homogenized in an ice-cold solution containing 50 mM Tris-HCl (pH 8.0), 150 mM NaCl, 1 mM EDTA, 1% Triton X-100, 1% sodium deoxycholate, 0.1% sodium dodecyl sulfate (SDS), supplemented with protease inhibitor cocktail (2 mM AEBSF, 1 mM EDTA, 130 µM bestatin plus 14 µM E-64 (proteases inhibitors), 1 µM leupeptin, 0.3 µM aprotinin). The samples were centrifuged at 12,000 × *g* for 12 min at 4 °C, and an aliquot of the supernatant to give a final protein concentration of 1 mg/ml was pre-incubated at 37°C in a reaction medium containing 20 mM PBS and 100 µM NADPH. Then, lucigenin was added (10 µM), and luminescence was evaluated in 10 one-second measurements at 30 s intervals at 37 °C (Varioskan Flash, Thermo Scientific, Loughborough, UK). The final result was presented as the sum of the luminescence obtained in 10 measurements and expressed as the relative light units (RLU) corrected by sample protein. The luminescence evaluated in the absence of NADPH was representative of basal $O_2^{\cdot-}$ production.

Renal Na^+-transporting ATPase activities

According to those described elsewhere, the activity of Na^+-transporting ATPases was quantified in homogenates from the *cortex corticis* and medulla (Vieira-Filho et al. 2014). Samples were homogenized in an isotonic solution containing 250 mM sucrose, 10 mM Hepes-Tris (pH 7.4), 2 mM EDTA, and 0.15 mg/mL

trypsin inhibitor in an ice bath. The ouabain-sensitive (Na^++K^+)ATPase and the ouabain-resistant Na^+-ATPase activities were quantified by measuring the ATP hydrolysis sensitive to ouabain and furosemide, respectively.

SDS-PAGE and Western blotting

The abundance of renal cortical proteins was measured by immunoblotting, as previously described (Vieira-Filho et al. 2014). The protein samples (80 µg) were separated by SDS polyacrylamide gel electrophoresis and transferred to a nitrocellulose membrane (G&E Healthcare, Buckinghamshire, UK). The non-specific binding sites of the membranes were blocked using 5% BSA or 5% non-fat milk solution, which were incubated overnight (4 °C) with the primary antibody (diluted in Tris-buffered saline containing 0.1% Tween, TBS-T) to the target protein. After washing with TBS-T, the membranes were incubated with the peroxidase-conjugated secondary antibody and then exposed to a peroxidase-sensitive chemiluminescent reagent (G&E Healthcare). The blots were visualized using an image acquisition system (Chemidoc MP, Bio-Rad, Hercules, CA).

The primary antibodies and their dilutions were: anti-TNF-α, 1:200 (IM-0406, Imuny Biotechnology, Campinas, Brazil); anti-interleukin 6, 1:200 (IM-0407, Imuny Biotechnology); anti-(pro)renin/renin, 1:500 (sc-133145, Santa Cruz Biotechnology, Santa Cruz, CA); anti-ACE1, 1:100 (sc-23908, Santa Cruz Biotechnology); Anti-ACE2, 1:1000 (ab108252, Abcam, Cambridge, UK); anti-AT_1R, 1:500 (sc-57036, Santa Cruz Biotechnology); anti-angiotensin II-type 2 receptor (AT_2R), 1:250 (sc-9040, Santa Cruz Biotechnology); anti-angiotensinogen, 1:500 (NBP1-30027, Novus Biologicals, Centennial, CO); anti-PKCα, 1:500 (sc-208, Santa Cruz Biotechnology); anti-PKCε, 1:500 (sc-214, Santa Cruz Biotechnology); anti-PKCζ, 1:500 (sc-216, Santa Cruz Biotechnology); anti-PKCλ, 1:250 (sc-1091, Santa Cruz Biotechnology); anti-PKA, 1:500 (sc-903, Santa Cruz Biotechnology); anti-(Na^++K^+)ATPase (α1 subunit), 1:1000 (A276, Sigma Aldrich); anti-β-actin, 1:5000 (sc-47778, Santa Cruz Biotechnology); anti- β-actin, 1:1000 (A5441, Sigma Aldrich). The molecular markers were provided by Sigma-Aldrich (GERPN800E) and Bio-Rad (161-0375). The original blots with the molecular markers are presented as supplementary figures (Fig. S1–Fig. S13).

Statistical analysis

The results are presented as mean ± SEM. First, the Shapiro-Wilk normality test evaluated whether the distribution of each parameter data was normal. Then, considering the Gaussian data distribution, the differences between groups was analysed using one-way ANOVA followed by Tukey's test. Differences were considered significant at $p<0.05$. The statistical analysis and graph drawing were performed using GraphPad Prism 6 software (version 6.01, GraphPad Software, Inc., San Diego, CA).

RESULTS

General metabolic data

After 24 h of paraquat administration, the rats showed a pronounced body weight loss, not observed in the tempol-treated group (Table I). Paraquat administration also led to decreased food (65%) and water (30%) intake, as well as increased diuresis (100%) and serum protein concentration (10%). Tempol treatment also prevented paraquat-induced changes in food intake, diuresis, and serum protein levels.

Renal and hepatic injury markers, systolic arterial pressure, and heart rate

Rats treated with paraquat presented with higher levels of serum creatinine (45%), AST (90%), and ALT (40%), as well as lower (50%) creatinine

Table I. General metabolic data, renal and hepatic function markers, systolic blood pressure, and heart rate.

	C (n = 8)	PQ (n = 8)	PQ+T (n = 7)
Body weight variation (g)	2.0 ± 1.7	–24.0 ± 4.0**	2.0 ± 6.0††
Food intake (g/100 g BW)	6.5 ± 0.3	2.3 ± 0.2***	6.1 ± 0.6†††
Water intake (mL/100 g BW)	13.9 ± 1.0	10.0 ± 0.9*	10.0 ± 1.3*
Diuresis (mL/100 g BW)	4.0 ± 0.2	8.0 ± 0.8***	5.3 ± 0.4††
Total serum protein (g/dL)	6.8 ± 0.1	7.5 ± 0.2*	6.7 ± 0.1†
Serum creatinine (mg/dL)	0.45 ± 0.02	0.65 ± 0.05**	0.67 ± 0.04**
Creatinine clearance (mL/min per 100 g BW)	0.91 ± 0.08	0.48 ± 0.06**	0.56 ± 0.06**
Proteinuria (mg/100 g BW)	35.8 ± 2.3	28.8 ± 3.5	29.1 ± 3.0
Serum AST (mg/dL)	76.8 ± 9.2	145.3 ± 6.2**	104.3 ± 15.8
Serum ALT (mg/dL)	40.0 ± 5.2	56.5 ± 1.6*	36.1 ± 4.0†
Systolic blood pressure (mmHg)	133 ± 3	145 ± 4*	136 ± 1
Heart rate (bpm)	405 ± 6	442 ± 9**	408 ± 7†

C: control rats; PQ: rats treated with paraquat; PQ+T: rats treated with paraquat that previously received tempol in drinking water. Food and water intake, diuresis and proteinuria correspond to a 24-h period. BW = body weight; AST = aspartate aminotransferase; ALT = alanine aminotransferase. BW = body weight. The results are expressed as mean ± SEM. *p<0.05, **p<0.01 and ***p<0.001 vs. C; †p<0.05, ††p<0.01 and †††p<0.001 vs. PQ (one-way ANOVA followed by Tukey's test compared means on each line).

clearance than the control group (Table I). Rats treated with paraquat plus tempol also presented higher serum creatinine and lower creatinine clearance than the control group; however, AST and ALT were utterly normalized. Proteinuria was not changed by paraquat administration or tempol treatment.

The SBP and heart rate were higher in rats submitted to paraquat administration than in the control group, while these changes were not observed in tempol-treated rats. We measured the SBP and heart rate values before paraquat (135 ± 1 mmHg; 409 ± 7 bpm) and paraquat plus tempol administrations (134 ± 1 mmHg; 406 ± 10 bpm). These values were compared with those recorded in the control rats at the same time (135 ± 3 mmHg; 413 ± 11 bpm) using one-way ANOVA followed by Tukey's test, and no difference was encountered among the three groups.

Renal and hepatic oxidative stress

Paraquat administration increased lipid peroxidation by more than 75% in the renal *cortex corticis*, renal medulla, and liver, while tempol treatment prevented these changes completely (Figure 1). Paraquat administration also induced the elevation of tissular reactive O_2 species (Figure 2) and $O_2^{\cdot-}$ formation (Figure 3a) in the *cortex corticis* and medulla. There were no differences between the C and PQ+T groups.

NADPH oxidase activity was also higher in the *cortex corticis* and medulla of paraquat-treated rats than in the control group (Figure 3b). In the cortex, paraquat increased NADPH oxidase activity by 100%, while the elevation was higher than 40% in the medulla. NADPH oxidase activity was not different between the PQ+T and C groups.

Effects of paraquat and tempol on renal Na^+-transporting ATPases

$(Na^+ + K^+)$ATPase activity was 70% higher in *cortex corticis* from paraquat-treated rats than in the C group, while it was 40% lower in the medulla (Figure 4a). $(Na^+ + K^+)$ATPase activity of the PQ+T group was not different from the C group in both

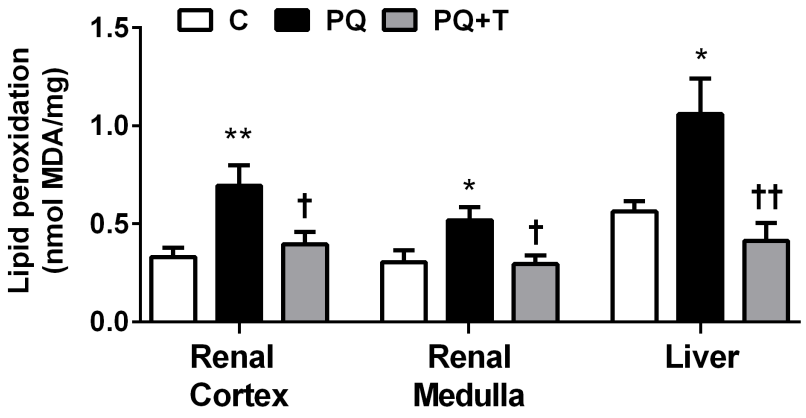

Figure 1. Tissue lipid peroxidation evaluated 24 h after paraquat administration. C: control rats; PQ: rats treated with paraquat; PQ+T: rats treated with paraquat that previously received tempol. Lipid peroxidation was evaluated by measuring the thiobarbituric acid reactive substances (TBARS) (MDA = malondialdehyde). The results are expressed as mean ± SEM (n 6–7). *p<0.05 and **p<0.01 vs. C; †p<0.05, and ††p<0.01 vs. PQ (one-way ANOVA followed by Tukey's test).

renal regions. Albeit paraquat promoted changes in (Na^++K^+)ATPase activity, the ROS-generating agent did not alter the protein content of the α1 subunit of the enzyme in renal tissue (data not shown).

Paraquat also induced opposite changes in Na^+-ATPase activity (Figure 4b) depending on the tissue region: in the *cortex corticis*, the Na^+-ATPase activity was 50% lower than in C rats, while it was 50% higher in the medulla. These changes were prevented by tempol treatment.

Inflammatory markers IL-6 and TNF-α in the renal cortex

To verify whether paraquat provoked renal pro-inflammatory effects, especially in the *cortex corticis*, we evaluated the renal content of IL-6 and TNF-α (Figure 5). IL-6 levels increased by 55% in PQ rats with respect to the C group, and TNF-α was 100% higher in the PQ compared to C rats. The administration of tempol did not prevent the augment of these inflammatory cytokines.

Intrarenal RAAS expression

The *cortex corticis* protein content of the RAAS components is depicted in Figure 6. Protein levels of angiotensinogen, prorenin, renin, isoform 1 of angiotensin-converting enzyme (ACE1), and isoform 2 of angiotensin-converting enzyme (ACE2) were similar among the experimental groups (Figure 6a–e, h). On the other hand, the renal content of angiotensin II-type 1 receptor (AT_1R) was 100% higher in rats treated with paraquat than in control rats (Figure 6f, h). Moreover, the AT_1R abundance did not differ between the tempol-treated and control groups. On the other hand, the abundance of angiotensin II-type 2 receptor (AT_2R) was not affected by paraquat administration; however, it increased by 100% with tempol treatment in rats that received paraquat (Figure 6g, h).

Protein kinase C and protein kinase A abundance

Since protein kinase C (PKC) and protein kinase A (PKA) are key components of the signaling pathways by which RAAS modulates the renal Na^+-transporting ATPases, the protein content of these intracellular mediators was evaluated (Figure 7). Paraquat did not affect the protein levels of any of the evaluated PKC isoforms, nor did it affect the PKA α-catalytic subunit levels. Nevertheless, paraquat rats treated with tempol presented nearly 50% higher renal cortical content of the PKC isoforms α and ε than control and paraquat-treated rats.

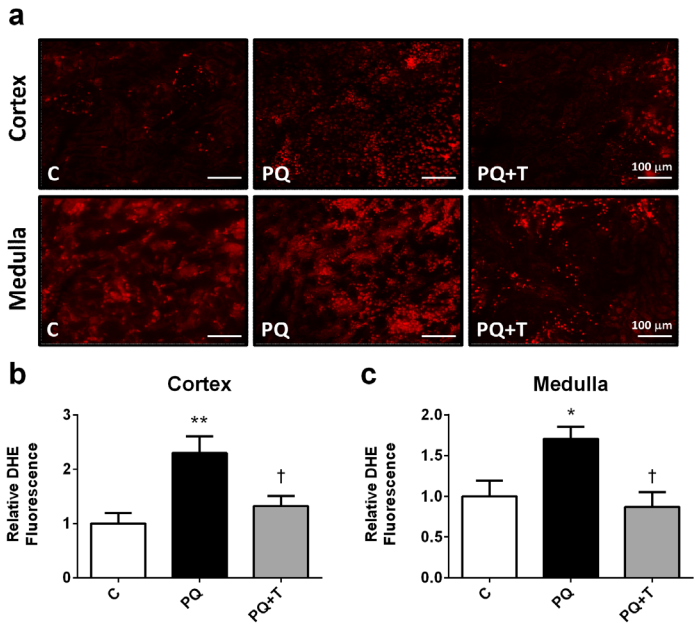

Figure 2. In situ evaluation of reactive O_2 species levels in renal tissue 24 h after paraquat administration. (Panel a) Representative images of dihydroethidium (DHE) fluorescence in *cortex corticis* and medulla. (Panel b) Relative DHE fluorescence evaluated in the cortex. (Panel c) Relative DHE fluorescence evaluated in the medulla. C: control rats; PQ: rats treated with paraquat; PQ+T: rats that received paraquat and that were previously treated with tempol. The results are expressed as mean ± SEM (n 4–5). **P*<0.05 and ***P*<0.01 vs. C; †*P*<0.05 vs. PQ (one-way ANOVA followed by Tukey's test).

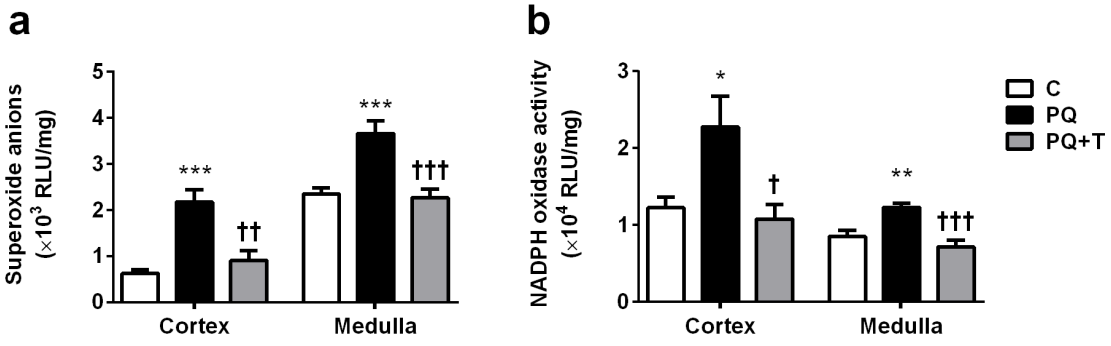

Figure 3. Basal $O_2^{\bullet-}$ production (a) and NADPH oxidase-stimulated $O_2^{\bullet-}$ formation (b). The assays were performed using *cortex corticis* and medulla 24 h after paraquat administration. C: control rats; PQ: rats treated with paraquat; PQ+T: rats treated with paraquat that previously received tempol. RLU = relative light units. The results are expressed as mean ± SEM (n = 5–8). *p<0.05, **p<0.01, and ***p<0.001 vs. C; †p<0.05, ††p<0.05, and †††p<0.001 vs. PQ (one-way ANOVA followed by Tukey's test).

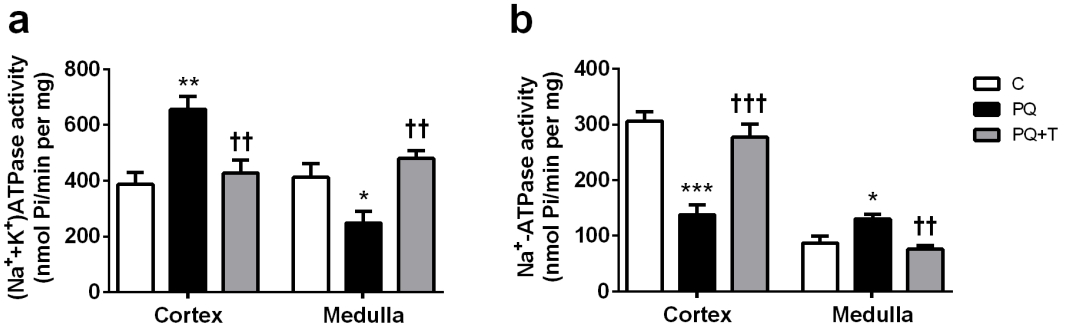

Figure 4. Na^+-transporting ATPases in *cortex corticis* and medulla. The ouabain-sensitive (Na^++K^+)ATPase (a) and the ouabain-resistant furosemide-sensitive Na^+-ATPase (b) were measured in renal tissue 24 h after paraquat administration. C: control rats; PQ: rats treated with paraquat; PQ+T: rats treated with paraquat that previously received tempol. P_i = inorganic phosphate. The results are expressed as mean ± SEM (n = 7–8 different membrane preparations). *p<0.05, ***p*<0.01, and ***p<0.001 vs. C; ††*P*<0.01 and †††*P*<0.001 vs. PQ (one-way ANOVA followed by Tukey's test).

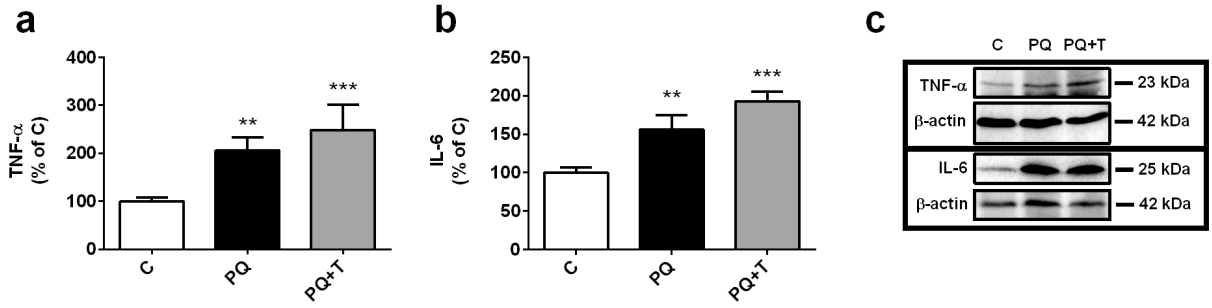

Figure 5. Tumor necrosis factor-α (TNF-α) (a) and interleukin-6 (IL-6) (b) immunodetection in the renal *cortex corticis* 24 h after paraquat administration. Panel c shows representative immunoblotting of TNF-α and IL-6, and the protein load control β-actin. C: control rats; PQ: rats treated with paraquat; PQ+T: rats treated with paraquat that previously received tempol. The results are expressed as mean ± SEM (n 6–8). ***P*<0.01 and ****P*<0.001 vs. C (one-way ANOVA followed by Tukey's test).

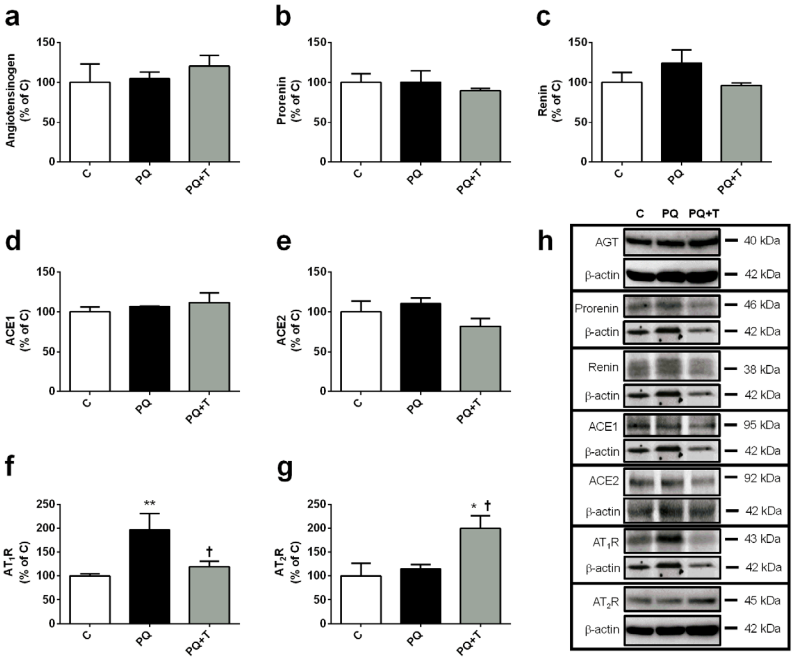

Figure 6. Immunodetection of several renin-angiotensin-aldosterone system (RAAS) components in the renal *cortex corticis* 24 h after paraquat administration. Panels a–g show the renal cortex immunoquantification of angiotensinogen, prorenin, renin, the isoforms 1 and 2 of angiotensin-converting enzyme (ACE1 and ACE2, respectively), and the angiotensin II-type 1 and 2 receptors (AT_1R, and AT_2R, respectively), as indicated in the corresponding ordinates. Panel h shows representative immunoblottings of the RAAS components and the loading control β-actin. C: control rats; PQ: rats treated with paraquat; PQ+T: rats treated with paraquat that previously received tempol. Bars show mean ± SEM (n 4–8). *p<0.05 and **p<0.01 vs. C; †p<0.05 vs. PQ (one-way ANOVA followed by Tukey's test).

DISCUSSION

In the present study, we demonstrated that the elevation of renal and hepatic markers of injury in paraquat-treated rats occurred in parallel with a substantial increase in $O_2^{\cdot-}$ formation (Figure 2) and lipid peroxidation (Figure 1), which could affect the lipid membrane moiety and membrane transporters in the kidney, especially in the cortex. Notably, the elevation of lipid peroxidation was more prominent in the renal *cortex corticis* than in the medulla (110% vs. 70%). This difference could be due to paraquat´s more significant impact on the elevation of basal $O_2^{\cdot-}$ production and NADPH oxidase activity in the renal cortex (Figure 3). Regarding the effect of tempol in the RAAS of rats that then received paraquat, the central and novel result is the upregulation of the AT_2R-associated pathway (Figure 6g), indicating that activation of this branch could antagonize the

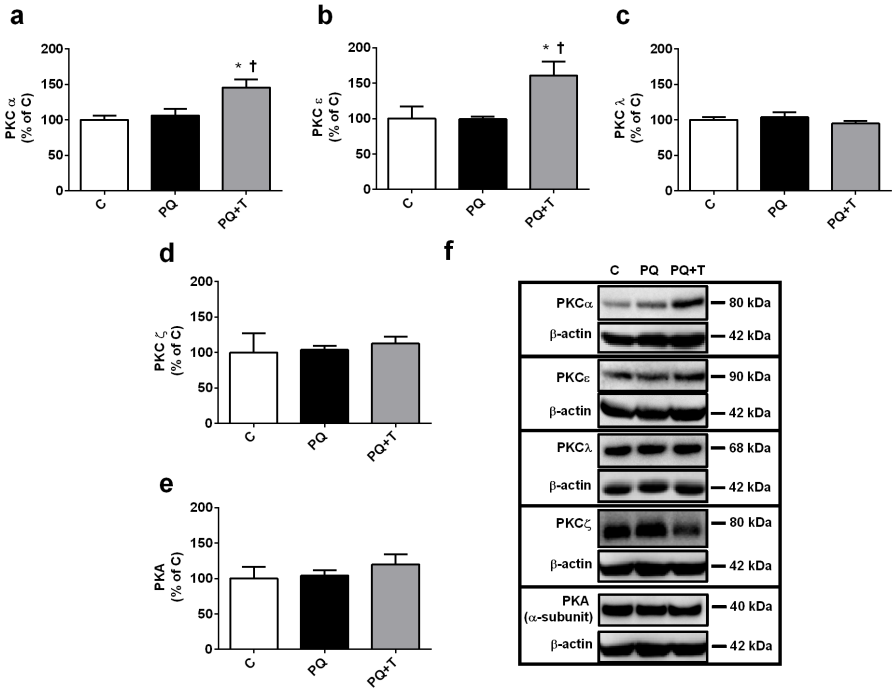

Figure 7. Immunodetection of protein kinase C (PKC) isoforms and protein kinase A (PKA) α-catalytic subunit in the renal cortex 24 h after paraquat administration. Panels a–e show immunoquantification of PKCα, PKCε, PKCλ, PKCξ and PKA α-catalytic subunit in renal *cortex corticis*. Panel f shows representative immunoblotting of PKC isoforms, PKA α-catalytic subunit, and the loading control β-actin. C: control rats; PQ: rats treated with paraquat; PQ+T: rats treated with paraquat that previously received tempol. The results are expressed as mean ± SEM (n = 5–8). *p<0.05 vs. C; †p<0.05 vs. PQ (one-way ANOVA followed by Tukey's test).

deleterious signaling starting at the level of upregulated AT_1R (Figure 6f).

Paraquat intoxication induces tubular injury characterized by tubular degeneration, renal vessel obstruction, and leukocyte infiltration (Mølck & Friis 1997). In the present study, the kidney inefficiency to avoid excessive fluid excretion could reflect tubular damage. A case study with two patients poisoned by paraquat reported that fractional Na^+ excretion was 40% higher than the filtered load (Vaziri et al. 1979). The unique *cortex corticis* vulnerability to paraquat-induced oxidative stress would be explained by several factors (Chan et al. 1996). After intoxication, the cortical concentration of paraquat increases because it exists as a divalent organic cation, actively secreted by proximal tubule cells using the polyvalent organic cation transport protein (Mølck & Friis 1997). Besides, the renal cortex has elevated blood flow and an intense oxidative metabolism (George et al. 2017), potentiating the paraquat-induced ROS formation.

In the medulla, the high rate of O_2 consumption of the thick ascending limb cells (Eveloff et al. 1981) would be crucial for an $O_2^{\cdot-}$-induced damage after paraquat administration; this would affect the Na^+ transporters involved in the hypertonicity of the interstitium (Rocha & Kokko 1973) and urine concentration. Possibly, the increased production of ROS and lipid peroxidation in paraquat-intoxicated rats that provoked inhibition of the medullary (Na^++K^+) ATPase are the central mechanisms of the copious urinary flux that we observed. The increased activity of the enzyme in proximal tubules possibly represents a compensatory process, facing the depletion of the liquid compartments by intense diuresis and depressed water intake. Increased activity of the RAS, as revealed by the upregulation of AT_1R levels, likely contributed to sustaining the production of $O_2^{\cdot-}$ due to activation of the AT_1R-mediated oxidative stress/angiotensinogen/RAS axis in the kidney (Vallés et al. 2020). As part of a vicious cycle, oxidative damage in the kidney could stimulate ROS

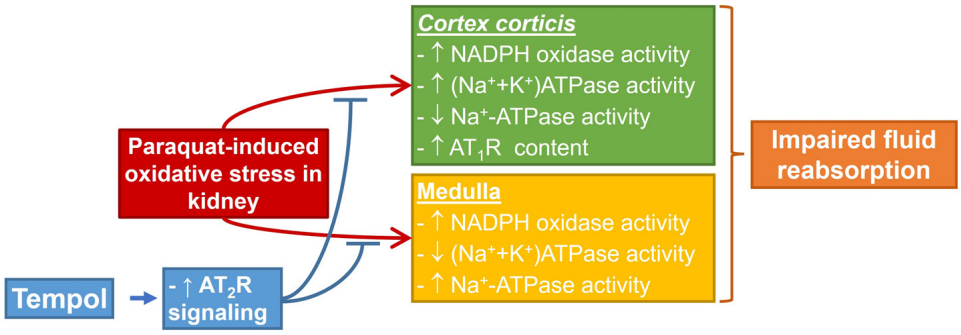

Figure 8. Graphical summary of the main effects of paraquat and tempol in the cortical and medullary renal regions.

production via the sympathetic nervous system (Cao et al. 2017).

Paraquat induces cellular and tissue damage by compromising cellular redox cycles and increasing ROS production in the kidney (Figure 2). The idea that the intense tissue damage provoked by paraquat relies on the elevated production of ROS receives support from the observation that the elevation of renal and hepatic markers of injury occurred parallel to the increased lipid peroxidation (Figure 1). Several studies show that antioxidant treatments benefit by alleviating paraquat-induced damage and promoting recovery (Han et al. 2014, Wei et al. 2014, Tan et al. 2015). In the present study, we demonstrated that tempol improved many parameters related to kidney function, such as (i) diuresis (Table I), (ii) tubular Na^+-transporting ATPases (Figure 4), and (iii) AT_1R levels (Figure 6). The normalization of the AT_1R implies the normalization of the above-mentioned AT_1R-mediated oxidative stress/angiotensinogen/RAAS axis.

Though the tempol-mediated protective mechanism over paraquat effects possibly results from its antioxidant effects, tempol seems to present additional beneficial effects, which deserve special mention in the AT_2R and PKCε – the novel isoform of PKC (Steinberg 2008) – upregulation (Figures 6 and 7). AT_2R upregulation may be linked to stimulating anti-inflammatory and antioxidative pathways (Arroja et al. 2016), and the observations of Figure 6 give support to the proposal that activation of the AT_2R-mediated signaling pathway by tempol underpins – at least in part – the cellular and molecular protection against the deleterious actions of paraquat in kidney elicited by upregulation of the AT_1R-associated pathway. Furthermore, the tempol-induced upregulation of PKCε, associated with protective responses against renal injury (Meier et al. 2007), could be evidence that the antioxidant response could be mediated through phosphorylations catalyzed by this kinase. The fact that tempol did not normalize the creatinine clearance (Table I) favors the idea that other mechanisms of damage not linked to $O_2^{\cdot-}$ formation are involved in the lesions that paraquat provokes in renal tissue, especially in glomeruli, where creatinine depuration occurs.

Although there is evidence that antioxidant treatments have anti-inflammatory effects (Tan et al. 2015), tempol did not prevent the elevation of renal content of TNF-α and IL-6 induced by the ROS-generating agent (Figure 5). This observation allows one to propose another mechanism for paraquat toxicity besides oxidative stress and explain the inability of tempol to prevent the elevation of serum creatinine levels (Table I), a marker of the renal lesion. Possibly, the paraquat effects on muscle metabolism (Mohamed et al. 2015) are insensitive to tempol, and the absence of tempol effects on pro-inflammatory

mediators indicates partial protection of renal function under challenge by paraquat. Thus, at least in part, paraquat induces renal injury by independent oxidative mechanisms (Huang et al. 2019). Paraquat could activate NF-kB signaling and, therefore, the production of the pro-inflammatory cytokines TNF-α and IL-6 in a ROS-independent manner, as observed in other pathologies (Bylund et al. 2007, Liu et al. 2016). Moreover, since plasma creatinine concentration and creatinine clearance remain abnormally modified in tempol-treated rats, it is likely that the pro-inflammatory cytokines formed by the ROS-independent signaling pathway provoke podocyte damage together with proximal tubular dysfunction (Mølck & Friis 1997, Milas et al. 2020). Support this proposal the elevated rate of paraquat uptake in proximal tubule cells (Chan et al.1996).

In conclusion, we demonstrated that the ROS-generating agent paraquat led to a significant urinary fluid loss that may be consequent to impaired Na^+ reabsorption in medullary regions, which is the critical mechanism for urine concentration, thus becoming a risk factor for vascular collapse and early death. Tubular damage in the proximal tubules due to intense lipid peroxidation could contribute to accentuated fluid loss. The upregulation of pro-hypertensive RAS components linked to the AT_1R signaling pathway may exacerbate renal injury. In a recent study (Lima et al. 2021), we demonstrated that increased NADPH oxidase activity and lipid peroxidation are central in renal tubular lesions, upregulation of cortical $(Na^+ + K^+)$ATPase, and genesis of arterial hypertension after ischemia followed by reperfusion (I/R). Thus, we propose that paraquat poisoning shares, at least in part, the same molecular mechanisms encountered in I/R, the leading cause of AKI. Additionally, the stimulus of pro-inflammatory cytokines in a ROS-independent manner could worsen the paraquat-provoked renal lesions. Figure 8 shows and summarizes the main results of the present study at the renal level.

This study presents some limitations that need to be addressed in the future. The study focuses on juvenile rats (Agoston 2017), and the effect of paraquat would be different immediately after weaning or in very old rats. In addition, other antioxidant compounds need to be tested besides tempol, a superoxide dismutase enzyme mimetic (Bernardy et al. 2017). For example, vitamins C and E ameliorate the toxicity of pesticides and herbicides in the liver, kidney, and testis (Magdy et al. 2016). Finally, our study focused on paraquat-induced renal damage and, possibly, other organs, such as the heart and liver, could be affected in a systemic paraquat-provoked hepatocardiorenal syndrome (Kazory & Ronco 2019, Crisóstomo et al. 2022).

Acknowledgments

The authors would like to thank Prof. Dayane Aparecida Gomes for providing access to the apparatus located in her laboratory (Multiuser Platform in Cellular and Molecular Biology – FACEPE 16/2012; grant number 1133-2.07/2012). The authors also thank Nielson T. Mello, Danielle Dutra, and Gloria Costa Sarmento for their technical support. This work was supported by research grants from the Conselho Nacional de Desenvolvimento Científico e Tecnológico (CNPq), Brazil (474004/2013-9, 311578/2019-5, 432468/20161); the Coordenação de Aperfeiçoamento de Pessoal de Nível Superior (CAPES) (88887.124150/2014-00 and 88887.320213/2019-00), Brazil; the -Fundação de Amparo a Ciência e Tecnologia de Pernambuco (FACEPE), Brazil (APQ-1072-2.07/15); and the Fundação de Amparo à Pesquisa do Estado do Rio de Janeiro (FAPERJ) (E-26/200.866/2021).

REFERENCES

AGOSTON DV. 2017. How to translate time? The temporal aspect of human and rodent biology. Front Neurol 8: 92. https://doi.org/10.3389/fneur.2017.00092.

AHMED LA, SHEHATA NI, ABDELKADER NF & KHATTAB MM. 2014. Tempol, a superoxide dismutase mimetic agent,

ameliorates cisplatin-induced nephrotoxicity through alleviation of mitochondrial dysfunction in mice. PLoS One 9: e108889. https://doi.org/10.1371/journal.pone.0108889.

ALBRECHT AJP, ALBRECHT LP & SILVA AFM. 2022. Agronomic implications of paraquat ban in Brazil. Adv Weed Sci 40: e020220040. https://doi.org/10.51694/AdvWeedSci/2022;40:seventy-five009.

ALGE JL, KARAKALA N, NEELY BA, JANECH MG, VELEZ JCQ & ARTHUR JM. 2013. Urinary angiotensinogen predicts adverse outcomes among acute kidney injury patients in the intensive care unit. Critical Care 17: R69. https://doi.org/10.1186/cc12612.

ALIZADEH S, ANANI-SARAB G, AMIRI H & HASHEMI M. 2022. Paraquat induced oxidative stress, DNA damage, and cytotoxicity in lymphocytes. Heliyon 8: e09895. https://doi.org/10.1016/j.heliyon.2022.e09895.

ARROJA MMC, REID E & MCCABE C. 2016. Therapeutic potential of the renin angiotensin system in ischaemic stroke. Exp Trans Stroke Med 8: 8. https://doi.org/10.1186/s13231-016-0022-1.

BEŁTOWSKI J, BORKOWSKA E, WÓJCICKA G & MARCINIAK A. 2007. Regulation of renal ouabain-resistant Na^+-ATPase by leptin, nitric oxide, reactive oxygen species, and cyclic nucleotides: implications for obesity-associated hypertension. Clin Exp Hypertens 29: 189–207. https://doi.org/10.1080/10641960701361585.

BERNARDY CCF, ZARPELON AC, PINHO-RIBEIRO FA, CALIXTO-CAMPOS C, CARVALHO TT, FATTORI V, BORGHI SM, CASAGRANDE R & VERRI WA JR. 2017. Tempol, a superoxide dismutase mimetic agent, inhibits superoxide anion-induced inflammatory pain in mice. Biomed Res Int 2017: 9584819. https://doi.org/10.1155/2017/9584819.

BYLUND J, MACDONALD KL, BROWN KL, MYDEL P, COLLINS LV, HANCOCK REW & SPEERT DP. 2007. Enhanced inflammatory responses of chronic granulomatous disease leukocytes involve ROS-independent activation of NF-κB. Eur J Immunol 37: 1087-1096. https://doi.org/10.1002/eji.200636651.

CAO W, LI A, LI J, WU C, CUI S, ZHOU Z, LIU Y, WILCOX CS & HOU FF. 2017. Reno-cerebral reflex activates the renin-angiotensin system, promoting oxidative stress and renal damage after ischemia-reperfusion injury. Antioxid Redox Signal 27: 415-432. https://doi.org/10.1089/ars.2016.6827.

CHAN BSH, LAZZARO VA, SEALE JP & DUGGIN GG. 1996. Characterisation and uptake of paraquat by rat renal proximal tubular cells in primary culture. Hum Exp Toxicol 15: 949-956. https://doi.org/10.1177/096032719601501202.

CHEVALIER RL. 2016. The proximal tubule is the primary target of injury and progression of kidney disease: role of the glomerulotubular junction. Am J Physiol Renal Physiol 311: F145-F161. https://doi.org/10.1152/ajprenal.00164.2016.

CRISÓSTOMO T, PARDAL MAE, HERDY SA, MUZI-FILHO H, MELLO DB, TAKIYA CM, LUZES R & VIEYRA A. 2022. Liver steatosis, cardiac and renal fibrosis, and hypertension in overweight rats: Angiotensin-(3-4)-sensitive hepatocardiorenal syndrome. Metabol Open 14: 100176. https://doi.org/10.1016/j.metop.2022.100176.

DA SILVEIRA KD ET AL. 2010. ACE2-angiotensin-(1-7)-Mas axis in renal ischaemia/reperfusion injury in rats. Clin Sci (Lond) 119: 385-394. https://doi.org/10.1042/CS20090554.

DEDEKE GA, OWAGBORIAYE FO, ADEMOLU KO, OLUJIMI OO & ALADESIDA AA. 2018. Comparative assessment on mechanism underlying renal toxicity of commercial formulation of roundup herbicide and glyphosate alone in male albino rat. Int J Toxicol 37: 285-295. https://doi.org/10.1177/1091581818779553.

DINIS-OLIVEIRA RJ, DUARTE JA, SÁNCHEZ-NAVARRO A, REMIÃO F, BASTOS ML & CARVALHO F. 2008. Paraquat poisonings: mechanisms of lung toxicity, clinical features, and treatment. Crit Rev Toxicol 38: 13-71. https://doi.org/10.1080/10408440701669959.

EVELOFF J, BAYERDÖRFFER E, SILVA P & KINNE R. 1981. Sodium-chloride transport in the thick ascending limb of Henle's loop. Oxygen consumption studies in isolated cells. Pflügers Archiv 389: 263-270. https://doi.org/10.1007/BF00584788.

FÉRAILLE E & DOUCET TA. 2001. Sodium-potassium-adenosinetriphosphatase-dependent sodium transport in the kidney: hormonal control. Physiol Rev 81: 345-418. https://doi.org/10.1152/physrev.2001.81.1.345.

GEORGE B, YOU D, JOY MS & ALEKSUNES LM. 2017. Xenobiotic transporters and kidney injury. Adv Drug Deliv Rev 166: 73-91. https://doi.org/10.1016/j.addr.2017.01.005.

HAN J, ZHANG Z, YANG S, WANG J, YANG X & TAN D. 2014. Betanin attenuates paraquat-induced liver toxicity through a mitochondrial pathway. Food Chem Toxicol 70: 100-106. https://doi.org/10.1016/j.fct.2014.04.038.

HAVASI A & BORKAN SC. 2011. Apoptosis and acute kidney injury. Kidney Int 80: 29-40. https://doi.org/10.1038/ki.2011.120.

HUANG J, NING N & ZHANG W. 2019. Effects of paraquat on IL-6 and TNF-α in macrophages. Exp Ther Med 17: 1783-1789. https://doi.org/10.3892/etm.2018.7099.

KAZORY A & RONCO C. 2019. Hepatorenal syndrome or hepatocardiorenal syndrome: Revisiting basic concepts in view of emerging data. Cardiorenal Med 9: 1-7. https://doi.org/10.1159/000492791.

KOBORI HI, NANGAKU M, NAVAR LG & NISHIYAMA A. 2007. The intrarenal renin-angiotensin system: from physiology to the pathobiology of hypertension and kidney disease. Pharmacol Rev 59: 251-287. https://doi.org/10.1124/pr.59.3.3.

LIMA NKS, FARIAS WRA, CIRILO MAS, OLIVEIRA AG, FARIAS JS, AIRES RS, MUZI-FILHO H, PAIXÃO ADO & VIEIRA LD. 2021. Renal ischemia-reperfusion leads to hypertension and changes in proximal tubule Na^+ transport and renin-angiotensin-aldosterone system: Role of NADPH oxidase. Life Sci 266: 118879. https://doi.org/10.1016/j.lfs.2020.118879.

LIU H, XU W, CHANG X, QIN T, YIN Y & YANG Q. 2016. 4,4'-diaponeurosporene, a C_{30} carotenoid, effectively activates dendritic cells *via* CD36 and NF-κB signaling in a ROS independent manner. Oncotarget 7: 40978-40991. https://doi.org/10.18632/oncotarget.9800.

LOWRY OH, ROSEBROUGH NJ, FARR AL & RANDAL RJ. 1951. Protein measurement with the Folin phenol reagent. J Biol Chem 193: 265-275. https://doi.org/10.1016/S0021-9258(19)52451-6.

MAGDY BW, MOHAMED FES, AMIN AS & RANA SS. 2016. Ameliorative effect of antioxidants (vitamins C and E) against abamectin toxicity in liver, kidney and testis of male albino rats. J Bas Appl Zool 77: 69-82. https://doi.org/10.1016/j.jobaz.2016.10.002.

MEIER M, MENNE J, PARK JK, HOLTZ M, GUELER F, KIRSCH T, SCHIFFER M, MENGEL M, LINDSCHAU C, LEITGES M & HALLER H. 2007. Deletion of protein kinase C-ε signaling pathway induces glomerulosclerosis and tubulointerstitial fibrosis *in vivo*. J Am Soc Nephrol 18: 1190-1198. https://doi.org/10.1681/ASN.2005070694.

MILAS O ET AL. 2020. Pro-inflammatory cytokines are associated with podocyte damage and proximal tubular dysfunction in the early stage of diabetic kidney disease in type 2 diabetes mellitus patients. J Diabetes Complications 34: 107479. https://doi.org/10.1016/j.jdiacomp.2019.107479.

MOECKEL GW. 2018. Pathologic perspectives on acute tubular injury assessment in the kidney biopsy. Semin Nephrol 38: 21-30. https://doi.org/10.1016/j.semnephrol.2017.09.003.

MOHAMED F ET AL. 2015. Mechanisms underlying early rapid increases in creatinine in paraquat poisoning. PLoS One 10: 0122357. https://doi.org/10.1371/journal.pone.0122357.

MØLCK AM & FRIIS C. 1997. The cytotoxic effect of paraquat to isolated renal proximal tubular segments from rabbits. Toxicol 122: 123-132. https://doi.org/10.1016/S0300-483X(97)00088-7.

OHKAWA H, OHISHI N & YAGI K. 1979. Assay for lipid peroxides in animal tissues by thiobarbituric acid reaction. Anal Biochem 95: 351-358. https://doi.org/10.1016/0003-2697(79)90738-3.

ROCAFULL MA, ROMERO FJ, THOMAS LE & DEL CASTILLO JR. 2011. Isolation and cloning of the K^+-independent, ouabain-insensitive Na^+-ATPase. Biochim Biophys Acta 1808: 1684-1700. https://doi.org/10.1016/j.bbamem.2011.02.010.

ROCAFULL MA, THOMAS LE & DEL CASTILLO JR. 2012. The second sodium pump: from the function to the gene. Pflugers Arch 463: 755-777. https://doi.org/10.1007/s00424-012-1101-3.

ROCHA AS & KOKKO JP. 1973. Sodium chloride and water transport in the medullary thick ascending limb of Henle. Evidence for active chloride transport. J Clin Invest 52: 612-623. https://doi.org/10.1172/JCI107223.

SACHSE A & WOLF G. 2007. Angiotensin II-induced reactive oxygen species and the kidney. J Am Soc Nephrol 18: 2439-2446. https://doi.org/10.1681/ASN.2007020149.

SINGH AP, JUNEMANN A, MUTHURAMAN A, JAGGI AS, SINGH N, GROVER K & DHAWAN R. 2012. Animal models of acute renal failure. Pharmacol Rep 64: 31-44. https://doi.org/10.1016/S1734-1140(12)70728-4.

STEINBERG SF. 2008. Structural basis of protein kinase C isoform function. Physiol Rev 88: 1341-1378. https://doi.org/10.1152/physrev.00034.2007.

SUKUMAR CA, SHANBHAG V & SHASTRY AB. 2019. Paraquat: The poison potion. Indian J Crit Care Med 23: S263-S266. https://doi.org/10.5005/jp-journals-10071-23306.

TAN D, WANG Y, BAI B, YANG X & HAN J. 2015. Betanin attenuates oxidative stress and inflammatory reaction in kidney of paraquat-treated rat. Food Chem Toxicol 78: 141-146. https://doi.org/10.1016/j.fct.2015.01.018.

UCHINO S ET AL. 2005. Acute renal failure in critically ill patients: a multinational, multicenter study. J Am Med Assoc (JAMA) 294: 813-818. https://doi.org/10.1001/jama.294.7.813.

VALLÉS PG, BOCANEGRA V, COSTANTINO VV, GIL LORENZO AF, EUGENIA BENARDON M & CACCIAMANI V. 2020. The renal antioxidative effect of losartan involves heat shock protein 70 in proximal tubule cells. Cell Stress Chaperones 25: 753-766. https://doi.org/10.1007/s12192-020-01119-8.

VAZIRI ND, NESS RL, FAIRSHTER RD, SMITH WR & ROSEN SM. 1979. Nephrotoxicity of paraquat in man. Arch Intern Med 139: 172-174. https://doi.org/10.1001/archinte.1979.03630390032014.

VIEIRA-FILHO LD, CABRAL EV, FARIAS JS, SILVA PA, MUZI-FILHO H, VIEYRA A & PAIXÃO ADO. 2014. Renal molecular mechanisms underlying altered Na^+ handling and genesis of hypertension during adulthood in prenatally undernourished rats. Br J Nutr 111: 1932-1944. https://doi.org/10.1017/S0007114513004236.

VIEYRA A, NACHBIN L, DIOS-ABAD E, GOLDFELD M, MEYER-FERNANDES JR & MORAES L. 1986. Comparison between calcium transport and adenosine triphosphatase activity in membrane vesicles derived from rabbit kidney proximal tubules. J Biol Chem 261: 4247-4255. https://doi.org/10.1016/S0021-9258(17)35654-5.

VIEYRA A, SILVA PA, MUZI-FILHO H, DICK CF, ARAUJO-DOS-SANTOS AL, DIAS J, VIEIRA-FILHO LD & PAIXÃO ADO. 2016. The role of the second Na^+ pump in mammals and parasites. In: Chakraborti S & Dhalla NS (Eds), Regulation of membrane Na^+-K^+ ATPase. Advances in biochemistry in health and disease, Winnipeg: Springer. v. 15: p. 93-112. https://doi.org/10.1007/978-3-319-24750-2_6.

WANG CT, NAVAR LG & MITCHELL KD. 2003. Proximal tubular fluid angiotensin II levels in angiotensin II-induced hypertensive rats. J Hypertens 21: 353-360. https://doi.org/10.1097/00004872-200302000-00027.

WEI T, TIAN W, LIU F & XIE G. 2014. Protective effects of exogenous β-hydroxybutyrate on paraquat toxicity in rat kidney. Biochem Biophys Res Commun 447: 666-671. https://doi.org/10.1016/j.bbrc.2014.04.074.

WHITTEMBURY G & PROVERBIO F. 1970. Two modes of Na extrusion in cells from guinea pig kidney cortex slices. Pflügers Arch 316: 1-25. https://doi.org/10.1007/bf00587893.

WUNNAPUK K, LIU X, PEAKE P, GOBE G, ENDRE Z, GRICE JE, ROBERTS MS & BUCKLEY NA. 2013. Renal biomarkers predict nephrotoxicity after paraquat. Toxicol Lett 222: 280-288. https://doi.org/10.1016/j.toxlet.2013.08.003.

YOON HE, KIM SJ, KIM SJ, CHUNG S & SHIN SJ. 2014. Tempol attenuates renal fibrosis in mice with unilateral ureteral obstruction: the role of PI3K-Akt-FoxO3a signaling. J Korean Med Sci 29: 230-237. https://doi.org/10.3346/jkms.2014.29.2.230.

YOUN CK, KIM J, JO ER, OH J, DO NY & CHO SI. 2016. Protective effect of tempol against cisplatin-induced ototoxicity. Int J Mol Sci 17: 1931. https://doi.org/10.3390/ijms17111931.

ZOBIOLE LHS, KRENCHINSKI FH, PEREIRA GR, RAMPAZZO PE, RUBIN RS & LUCIO FR. 2018. Management programs to control Conyza spp. in pre-soybean sowing applications. Planta Daninha 36: 1-8. https://doi.org/10.1590/S0100-83582018360100076.

How to cite

CIRILO MAS, SANTOS VBS, LIMA NKS, MUZI-FILHO H, PAIXÃO ADO, VIEYRA A & VIEIRA LD. 2024. Reactive oxygen species impair Na^+ transport and renal components of the renin-angiotensin-aldosterone system after paraquat poisoning. An Acad Bras Cienc 96: e20230971. DOI 10.1590/0001-3765202420230971.

Manuscript received on August 28, 2023;
accepted for publication on November 14, 2023

MARRY A.S. CIRILO[1]
https://orcid.org/0000-0003-1525-7741

VALÉRIA B.S. SANTOS[1]
https://orcid.org/0000-0003-1899-4624

NATÁLIA K.S. LIMA[1]
https://orcid.org/0000-0002-7140-8156

HUMBERTO MUZI-FILHO[2,3,4]
https://orcid.org/0000-0002-9183-1699

ANA D.O. PAIXÃO[1]
https://orcid.org/0000-0003-1129-3032

ADALBERTO VIEYRA[2,3,4,5]
https://orcid.org/0000-0002-8009-7273

LEUCIO D. VIEIRA[1,3]
https://orcid.org/0000-0002-6041-1720

[1]Federal University of Pernambuco, Department of Physiology and Pharmacology, Professor Moraes Rego Ave., University City, 50670-901 Recife, PE, Brazil

[2]Federal University of Rio de Janeiro, Center for Research in Precision Medicine, First Floor, Carlos Chagas Filho Institute of Biophysics, Carlos Chagas Filho Ave., University City, 21941-904 Rio de Janeiro, RJ, Brazil

[3]Federal University of Rio de Janeiro, National Center for Structural Biology and Bioimaging/CENABIO, 373 Carlos Chagas Filho Ave., University City, 21941-902 Rio de Janeiro, RJ, Brazil

[4]National Institute of Science and Technology in Regenerative Medicine-REGENERA, 373 Carlos Chagas Filho Ave., University City, 21941-902 Rio de Janeiro, RJ, Brazil

[5]Grande Rio University, 1160 Professor José de Souza Herdy Street, Building C, Second Floor, 25071-202 Duque de Caxias, RJ, Brazil

Correspondence to: **Adalberto Vieyra / Leucio D. Vieira**
E-mail: avieyra@biof.ufrj.br / leucio.vieirafo@ufpe.br

Author contributions

MASC, HM-F, ADOP, AV, and LDV conceived and designed the study. MASC, VBSS, NKSL, and HM-F contributed running the laboratory work, analysis of the data, and drafted the paper. MASC, VBSS, NKSL, HM-F, ADOP, AV, and LDV contributed to critical reading of the manuscript. HM-F, ADOP, AV, and LDV supervised the laboratory work and obtained funding. All the authors participated of the final writing of the paper and approved the submission.